The American Journal of Pathology, Vol. 184, No. 5, May 2014

The American Journal of
PATHOLOGY
ajp.amjpathol.org

VASCULAR BIOLOGY, ATHEROSCLEROSIS, AND ENDOTHELIUM BIOLOGY

Endothelial NLRP3 Inflammasome Activation and Enhanced Neointima Formation in Mice by Adipokine Visfatin

Min Xia, Krishna M. Boini, Justine M. Abais, Ming Xu, Yang Zhang, and Pin-Lan Li

From the Department of Pharmacology & Toxicology, Medical College of Virginia, Virginia Commonwealth University, Richmond, Virginia

Accepted for publication January 30, 2014.

Address correspondence to Pin-Lan Li, M.D., Ph.D., Department of Pharmacology & Toxicology, Medical College of Virginia Campus, Virginia Commonwealth University, Richmond, VA 23298. E-mail: pli@vcu.edu.

Inflammasomes serve as an intracellular machinery to initiate inflammatory response to various danger signals. The present study tested whether an inflammasome centered on nucleotide oligomerization domain-like receptor protein 3 (NLRP3) triggers endothelial inflammatory response to adipokine visfatin, a major injurious adipokine during obesity. NLRP3 inflammasome components were abundantly expressed in cultured mouse microvascular endothelial cells, including NLRP3, apoptosis-associated speck-like protein, and caspase-1. These NLRP3 inflammasome molecules could be aggregated to form an inflammasome complex on stimulation of visfatin, as shown by fluorescence confocal microscopy and size exclusion chromatography. Correspondingly, visfatin significantly increased caspase-1 activity and IL-1β release in microvascular endothelial cells, indicating an activation of NLRP3 inflammasomes. In animal experiments, direct infusion of visfatin in mice with partially ligated left carotid artery were found to have significantly increased neointimal formation, which was correlated with increased NLRP3 inflammasome formation and IL-1β production in the intima. Further, visfatin-induced neointimal formation, endothelial inflammasome formation, and IL-1β production in mouse partially ligated left carotid artery were abolished by caspase-1 inhibition, local delivery of apoptosis-associated speck-like protein shRNA or deletion of the *ASC* gene. In conclusion, the formation and activation of NLRP3 inflammasomes by adipokine visfatin may be an important initiating mechanism to turn on the endothelial inflammatory response leading to arterial inflammation and endothelial dysfunction in mice during early stage obesity. *(Am J Pathol 2014, 184: 1617–1628; http://dx.doi.org/10.1016/j.ajpath.2014.01.032)*

Obesity is a major risk factor for cardiovascular disease and has been strongly associated with endothelial dysfunction and coronary atherosclerosis. Obese patients have significantly elevated morbidity and mortality due to coronary artery disease.[1] However, weight loss can decrease cardiovascular risk, improve endothelial function, and protect coronary arteries from atherosclerotic injury. However, mechanisms underlying obesity-associated coronary atherosclerotic injury and endothelial dysfunction are not fully understood. Numerous studies have reported a critical role of vascular inflammation in the development of coronary atherosclerosis, which has been characterized as an inflammatory disease.[2–6] To date, the precise mechanism that mediates the early inflammatory responses of endothelial cells (ECs) during obesity remains unknown.

Recently, the inflammasome as an intracellular inflammatory machinery has been reported to switch on the inflammatory response of tissues or organs to various danger signals.[7,8] Among different types of inflammasomes, the nucleotide oligomerization domain (Nod)-like receptor family pyrin domain containing 3 (NLRP3) inflammasome is well characterized in a variety of mammalian cells, especially as a receptor for endogenous danger signals such as ATP, cholesterol crystal, β-amyloid, and monosodium urate.[2,9–14] The NLRP3 inflammasome is characteristic of a proteolytic complex mainly composed of NLRP3, the adaptor protein apoptosis-associated speck-like protein (ASC), and caspase-1. On stimulation, NLRP3 inflammasomes oligomerize to form large multimolecular complexes

Supported by the NIH grants HL-57244, HL-075316, DK54927, and HL-091464 (P.-L.L.).

Disclosures: None declared.

http://dx.doi.org/10.1016/j.ajpath.2014.01.032

that control the caspase-1 activity and subsequent bioactive IL-1β production.[10,15–18] More recently, NLRP3 inflammasomes have been implicated in the development of obesity and insulin resistance.[11] For example, the consumption of a high-fat diet (HFD) has been considered as critical contributor to type 2 diabetes, and NLRP3 inflammasome might be an important pathway of HFD mediating insulin resistance leading to inflammation.[19] These findings led us to wonder whether activation of NLRP3 inflammasome is an initiating mechanism for obesity-induced endothelial inflammatory responses.

Adipose tissue as an active metabolic tissue secretes multiple metabolically important proteins known as 'adipokines.'[20,21] Visfatin is a newly identified adipokine and a major injurious factor during obesity-associated diseases, including diabetes,[22] carotid and coronary atherosclerosis,[23,24] and chronic kidney disease.[25,26] Visfatin has also been considered as a proinflammatory adipokine to promote endothelial inflammation and injury.[27,28] The present study was designed to test the hypothesis that activation of NLRP3 inflammasomes is one of the important mechanisms that mediate endothelial inflammatory response to visfatin during early-stage obesity. We used a series of molecular and physiological approaches both *in vitro* and *in vivo* to test this hypothesis.

Materials and Methods

Cell Culture and Treatment

The mouse microvascular EC (MVEC; also known as established murine microvascular EC) line was purchased from ATCC (Manassas, VA). This cell line was originally isolated from mouse hemangioendothelioma. These MVECs were cultured in Dulbecco's modified Eagle's medium (Gibco, Carlsbad, CA), supplemented with 10% fetal bovine serum (Gibco) and 1% penicillin–streptomycin (Gibco) in humidified 95% air and 5% CO_2 mixture at 37°C. Cells were passaged by trypsinization (Trypsin/EDTA; Sigma, St. Louis, MO), followed by dilution in Dulbecco's modified Eagle's medium that contained 10% fetal bovine serum. Cells were used for experiments between passages 6 and 13. Cells were treated with 2 μg/mL visfatin (BioVision, Mountain View, CA) for indicated hours. Because the optimum response of inflammasome activation was observed after 4-hour visfatin stimulation, the same treatment was used in all experiments of the present study if not otherwise mentioned. To inhibit caspase-1 activity, cells were pretreated with 1 mmol/L Z-WEHD-FMK (WEHD; R&D Systems, Minneapolis, MN) for 30 minutes.

RNA Interference of ASC

siRNAs were commercially available (Qiagen, Valencia, CA). The sequence for *ASC* siRNA is 5′-AAGGCCGTGAGTTTC-TACCT-3′, which was confirmed to be effective in silencing *ASC* gene in different cells by the company. The scrambled smRNA (5′-AATTCTCCGAACGTGTCACGT-3′) has been also confirmed as nonsilencing double-stranded RNA and was used as control in the present study. Transfection of siRNA was performed with the siLentFect Lipid Reagent (Bio-Rad, Hercules, CA) according to the manufacturer's instructions.

RT-PCR

Total RNA from cells was extracted with TRIzol reagent (Invitrogen, Carlsbad, CA) according to the manufacturer's protocol. One-microgram aliquots of total RNA from each sample were reverse-transcribed into cDNA by using a first-strand cDNA synthesis kit (Bio-Rad). Equal amounts of the reverse transcriptional products were subjected to PCR amplification on a Bio-Rad iCycler system (Bio-Rad). The primers used in this study were synthesized by Operon (Huntsville, AL), and the sequences were as follows: NLRP3 sense, 5′-TACGGCCGTCTACGTCTTCT-3′; NLRP3 antisense, 5′-CGCAGATCACACTCCTCAAA-3′; ASC sense, 5′-ACAGAAGTGGACGGAGTGCT-3′; ASC antisense, 5′-CTCCAGGTCCATCACCAAGT-3′; caspase-1 sense, 5′-CACAGCTCTGGAGATGGTGA-3′; caspase-1 antisense, 5′-TCTTTCAAGCTTGGGCACTT-3′; and β-actin sense 5′-TCGCTGCGCTGGTCGTC-3′; β-actin antisense 5′-GGC-CTCGTCACCCACATAGGA-3′.

Confocal Microscopic Analysis

For confocal analysis of inflammasome molecules in MVECs, cultured cells were grown on glass coverslips, stimulated or unstimulated, and fixed in 4% paraformaldehyde in PBS for 15 minutes. After being permeablized with 0.1% Triton X-100/PBS and rinsed with PBS, the cells were incubated overnight at 4°C with goat anti-NLRP3 (1:200; Abcam, Cambridge, MA) and rabbit anti-ASC (1:50; Enzo, PA), or rabbit anti–caspase-1 (1:100; Abcam). To colocalize inflammasome molecules in the mouse coronary artery, double-immunofluorescence staining was performed with frozen tissue slides. After fixation, the slides were incubated overnight at 4°C with goat anti-NLRP3 (1:200) and rabbit anti-ASC (1:50) or with anti–caspase-1 (1:100). After washing, these slides probed with primary antibodies were incubated with Alexa 488- or Alexa 555-labeled secondary antibodies for 1 hour at room temperature. The slides were mounted and subjected to examinations by using a confocal laser scanning microscope (Fluoview FV1000; Olympus, Tokyo, Japan), with photos being taken, and the colocalization of NLRP3 with ASC or caspase-1 was analyzed by the Image Pro Plus version 6.0 software (Media Cybernetics, Bethesda, MD). These summarized colocalization efficiency data were expressed as Pearson correlation coefficient as we described previously.[28]

Immunocytochemical Analysis

For immunocytochemical analysis, MVECs grown on glass coverslips were quickly washed by PBS and fixed in 4%

paraformaldehyde in PBS for 15 minutes. Then cells were permeabilized by washing with a PBS-Tween 20 buffer twice and followed by 1% bovine serum albumin blocking for 30 minutes before the primary antibody incubation (1:200). After 1 hour of incubation at room temperature, the slides were washed and incubated with biotinylated IgG secondary antibody (1:500) for 1 hour and then with streptavidin-horseradish peroxidase for 30 minutes at room temperature. After 1 minute of diaminobenzidine staining, the slides were rinsed and counterstained with hematoxylin. The slides were then mounted and observed under a microscope.

Western Blot Analysis

Protein from cell lysate was run on a SDS-PAGE gel, transferred into polyvinylidene difluoride membrane, and blocked. Then the membrane was probed with primary antibodies against NLRP3, ASC, or caspase-1 (1:500 dilution) overnight at 4°C, followed by incubation with horseradish-labeled IgG. The immunoreactive bands were detected by chemiluminescence methods and visualized on Kodak Omat film. β-Actin was reprobed to serve as a loading control. The intensity of the bands was quantified by densitometry with the use of ImageJ software version 1.44p (NIH, Bethesda, MD).

SEC

After visfatin treatment, cells were homogenized with the following protein extraction buffer: 20 mmol/L 4-(2-hydroxyethyl)-1-piperazineethanesulfonic acid-KOH (pH 7.5), 10 mmol/L KCl, 1.5 mmol/L $MgCl_2$, 1 mmol/L Na EDTA, 1 mmol/L Na EGTA, and 1 × protease inhibitor cocktail set I (Calbiochem, Gibbstown, NJ). Samples were then centrifuged at 18,000 × *g* for 10 minutes at 4°C and run on a Sepharose 6 size-exclusion chromatography (SEC) column with the following buffer: 50 mmol/L Tris (pH 7.4), 150 mmol/L NaCl, 1% octylglucoside, and 1× protease inhibitor cocktail. Fractions (200 μL) were collected, starting at the void volume time. Five times sample buffer was added directly to the fractions, heated at 95°C for 5 minutes, and then resolved in SDS-PAGE gels followed by Western blot analysis. Protein standards were run on a column under identical conditions, and the fractions were analyzed with absorbance at 280 nm.

Caspase-1 Activity and IL-1β Production Assay

After visfatin treatment, cells were harvested and homogenized to extract proteins for caspase-1 activity assay by using a commercially available kit (Biovision). These data were expressed as the fold change compared with control cells. In addition, the cell supernatant was also collected to measure the IL-1β production by a mouse IL-1β ELISA kit (Bender Medsystems, Burlingame, CA) according to the protocol described by the manufacturer.

ESR Spectrometric Detection of O_2^-

Electromagnetic spin resonance (ESR) detection of O_2^- was also performed as we described previously.[28,29] In brief, after visfatin treatment, MVECs were gently collected in modified Krebs/HEPES buffer that contained 25 mmol/L deferroximine (metal chelator). Approximately 1×10^6 MVECs were mixed with 1 mmol/L spin-trap compound, 1-hydroxy-3-methoxycarbonyl-2,2,5,5-tetrame-thyl-pyrrolidine, in the presence or absence of 100 U/mL polyethylene glycol-conjugated superoxide dismutase. The cell mixture loaded in glass capillaries was immediately analyzed by ESR (Noxygen Science Transfer & Diagnostics GmbH, Denzlingen, Germany) for production of O_2^- at each minute for 10 minutes. The superoxide dismutase-inhibitable signals were normalized by protein concentration and compared among different experimental groups.

Partial Carotid Ligation and Osmotic Pump Implantation

Eight-week-old male C57BL/6J wild-type and $Asc^{-/-}$ mice were used.[12] All protocols were approved by the Institutional Animal Care and Use Committee of Virginia Commonwealth University. Partial carotid ligation surgery was performed as previously reported by others.[30,31] In brief, animals were sedated with 2% isoflurane that was provided through a nose cone. Next, a ventral midline incision of 4 to 5 mm was made in the neck. With the use of blunt dissection, muscle layers were separated with curved forceps to expose the left carotid artery (LCA). Three of four branches of the LCA (left external carotid, internal carotid, and occipital arteries) were ligated by using a 6-0 silk suture. The superior thyroid artery was left intact, providing the sole source for blood circulation. The incision was then closed, and the animals were kept on a heating pad until they gained consciousness. In the visfatin infusion group, the osmotic pump (model 2002; Alzet, Cupertino, CA) filled with 20 ng/kg per day of visfatin was implanted subcutaneously, and the catheter was inserted into the external jugular vein. In another group, mice were injected intraperitoneally with WEHD, a caspase-1 inhibitor, at a dosage of 1 mg/kg per day before implantation of the visfatin pump. Fourteen days after partial ligation, animals were sacrificed by cervical dislocation after the administration of anesthesia. Blood samples were collected; LCAs and right carotid arteries were then harvested for immunohistochemistry, dual fluorescence staining, and confocal analysis.

Gene Transfection in Mouse Carotid Artery by Ultrasound-Microbubble Technique

Plasmid DNA or shRNA (200 μg) was freshly prepared in 300 μL of saline with 20% microbubble (Optison; GE Healthcare, Chalfont St. Giles, UK). After anesthesia by 2% of isoflurane, the LCA was exposed by a midline incision, and then the left femoral vein was exposed as well. The

plasmid mixture was directly injected into the femoral vein. Simultaneously, transthoracic ultrasound insonation (Sonitron 2000; Rich-Mar, Inola, OK) was performed through a 6-mm diameter probe with an input frequency of 1 MHz, an output intensity of 1.0 to 2.0 W/cm^2, a pulse duty ratio of 10% to 50% for a total of 180 seconds with 30-second intervals. After closing the wound, the mouse remained on the heating board until recovery.

In Vivo Imaging of Gene Expression in Mouse Carotid Artery

To monitor the efficiency of gene expression through somatic plasmid transfection, mice were anesthetized with 0.7% to 1.5% isoflurane, and an aqueous solution of 150 mg/kg luciferin was intraperitoneally injected 5 minutes before imaging. The anesthetized mice were imaged with the IVIS200 *in vivo* imaging system (Xenogen, Alameda, CA). Photons emitted from luciferase-expressing cells within the animal body and transmitted through tissue layers were quantified over a defined period of time that ranged up to 5 minutes by using the software program Living Image (Xenogen) as an overlay on an Igor program version 2.6 (WaveMetrics, Lake Oswego, OR).

Animals

C57BL/6J mice (8 weeks of age, male; The Jackson Laboratory, Bar Harbor, ME) were fed a normal diet (ND) or a HFD (Dyets Inc., Bethlehem, PA) for 10 weeks to induce obesity as we described previously.[32] In another group, mice were injected intraperitoneally with WEHD, a caspase-1 inhibitor, at a dosage of 1 mg/kg per day before the treatment with HFD. At the end point, blood samples were collected, these mice were sacrificed, and heart tissues were harvested for dual fluorescence staining and confocal analysis. All protocols were approved by the Institutional Animal Care and Use Committee of Virginia Commonwealth University.

Immunohistochemistry

Formalin-fixed, paraffin-embedded heart tissue sections (4 μm) were stained with rabbit anti-visfatin (1:50; Abcam) and goat anti-IL1β (1:50; R&D Systems) overnight at 4°C after a 20-minute wash with 3% H_2O_2 and 30-minute blocking with serum. The slides were sequentially treated with CHEMICON IHC Select horseradish peroxidase/diaminobenzidine Kit (EMD Millipore, Billerica, MA) according to the protocol described by the manufacturer. Finally, the slides were counterstained with hematoxylin. Negative controls were prepared by leaving out the primary antibodies.

Statistical Analysis

Data are presented as means ± SEM. Significant differences between and within multiple groups were examined with analysis of variance for repeated measures, followed by

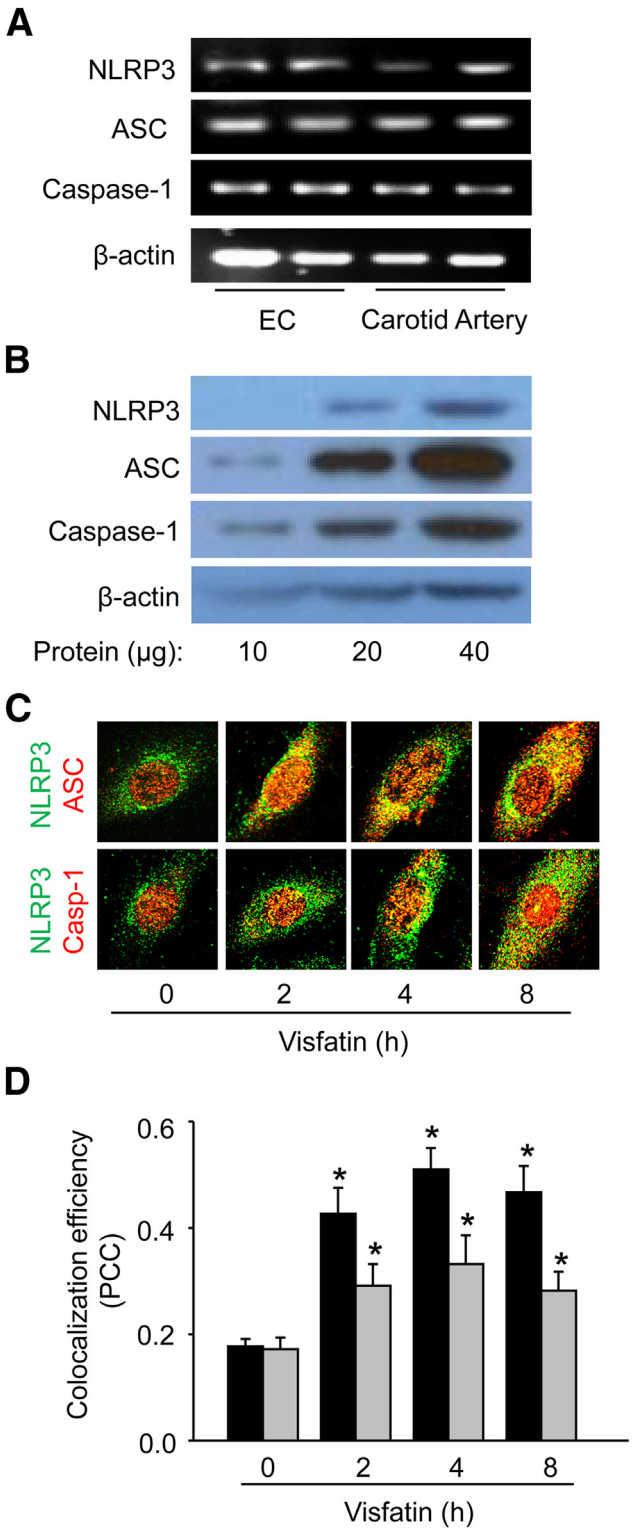

Figure 1 Visfatin increases NLRP3 inflammasome formation in MVECs. **A:** RT-PCR gel images show the expression of NLRP3, ASC, and caspase-1 in cultured MVECs and in carotid arteries. **B:** Western blot analysis shows protein expression of NLRP3, ASC, and caspase-1 in MVECs. **C:** Representative confocal fluorescence images depict the effect of visfatin on the colocalization of NLRP3 with ASC or caspase-1. **D:** Summarized data show the colocalization efficiency of NLRP3 with ASC (black bars) or NLRP3 with caspase-1 (gray bars). Data are expressed as means ± SEM; $n = 6$ (**A**, **B**, and **D**). *$P < 0.05$ versus untreated control group. Casp-1, caspase-1.

Duncan's multiple-range test. $P < 0.05$ was considered statistically significant.

Results

Visfatin Induces the NLRP3 Inflammasome Formation in MVECs

With the use of cultured mouse MVECs, we first characterized the formation of NLRP3 inflammasomes. RT-PCR analysis detected NLRP3, ASC, and caspase-1 mRNAs in MVECs (Figure 1A). The protein expression of these inflammasome components were confirmed by Western blot analysis (Figure 1B).

We next analyzed the inflammasome formation in MVECs by SEC and confocal microscopy. As shown in Figure 1C, the colocalization of NLRP3 with ASC or caspase-1 was increased in a time-dependent manner, indicating the aggregation or assembly of these inflammasome molecules. The Pearson correlation coefficient of NLRP3 with ASC or caspase-1 was summarized to represent the colocalization efficiency (Figure 1D). Such colocalization of NLRP3 molecules suggested the formation of NLRP3 inflammasomes in MVECs on visfatin stimulation. The maximum colocalization level was observed after 4-hour treatment of visfatin in MVECs; therefore, the same visfatin treatment was used in the rest of experiments if not otherwise mentioned.

To further confirm the NLRP3 inflammasome formation in response to visfatin, we next analyzed the assembly of NLRP3 inflammasome proteins as a complex in MVECs by SEC. Total proteins from MVECs were eluted through a Sepharose 6 SEC column, and all of the proteins were separated into different fractions according to their size and were detected by Western blot analysis (Figure 2A). It was observed that the specific bands for NLRP3, ASC, and caspase-1 were located in the low-molecular weight fractions under control conditions. However, on stimulation of visfatin for 4 hours, these bands specific to inflammasome components migrated into high-molecular weight factions, which were termed inflammasome fractions (Figure 2B); however, such migration was not found in cells transfected with ASC siRNA, indicating the aggregation or assembly of these inflammasome molecules, namely, the formation of NLRP3 inflammasome complex in MVECs. Moreover, visfatin treatment increased total protein expression of inflammasome components in MVECs. On Asc siRNA transfection before the addition of visfatin, a clear decrease in large inflammasome protein complex was observed in the high-molecular weight fractions. The intensity of these bands was quantified by ImageJ software and summarized (Figure 2C).

Visfatin Increases Caspase-1 Activity and IL-1β Production in MVECs

Visfatin significantly increased expression of active caspase-1 (20 kDa), indicating increased cleavage of pro—caspase-1 into

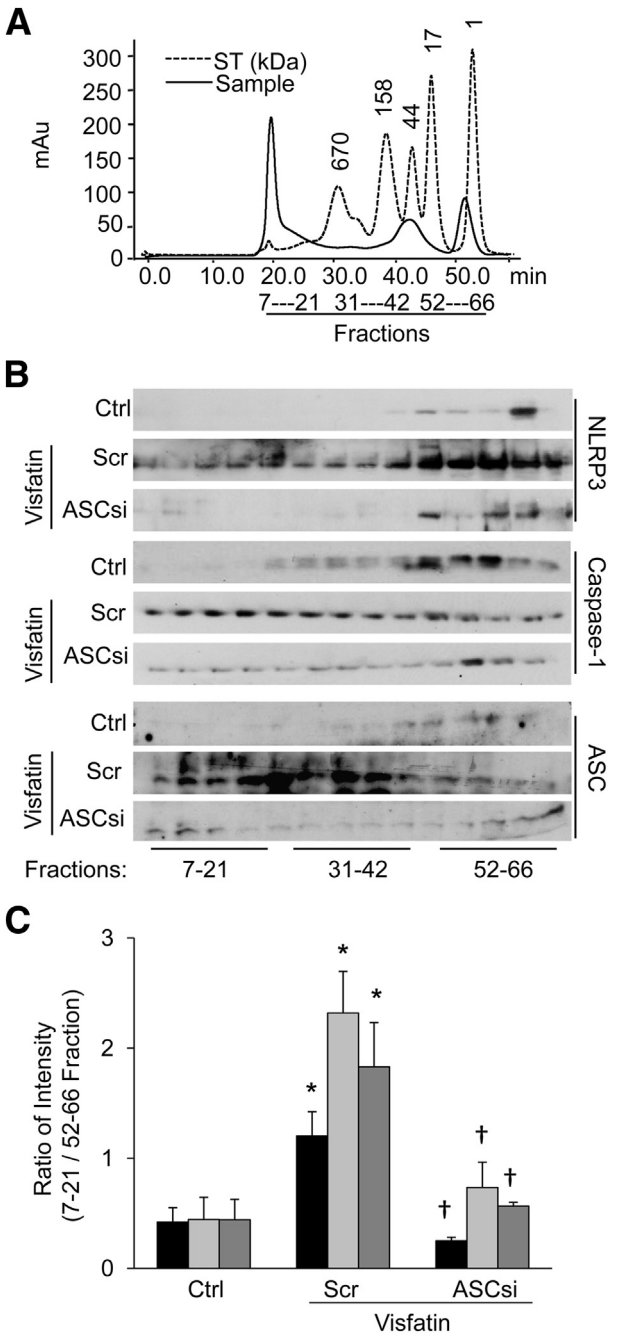

Figure 2 Distribution of inflammasome components after size-exclusion chromatography in MVECs. **A:** Elution profile of proteins from both standard and MVEC samples at an absorbance of 280 nm. Molecular mass of the samples were determined by comparison to a gel filtration standard. **B:** Western blot analysis of protein fractions obtained from untreated, visfatin, Asc siRNA-treated MVECs probed with anti-NLRP3, ASC, and caspase-1 antibodies. **C:** Data summary shows the band intensities measured from the inflammasome complex fractions (fractions 7 to 21) of NLRP3 (black bars), ASC (light gray bars), and caspase-1 (dark gray bars). Data are expressed as means ± SEM; $n = 6$ (**C**). $^{*}P < 0.05$ versus Ctrl group; $^{\dagger}P < 0.05$ versus Scr + visfatin group. ASCsi, ASC siRNA; Ctrl, control; Scr, scramble.

bioactive caspase-1 (Figure 3, A and B). We also noticed that visfatin did not decrease protein expression of pro—caspase-1, which could be due to up-regulation of pro—caspase-1 protein synthesis. Consistently, visfatin significantly

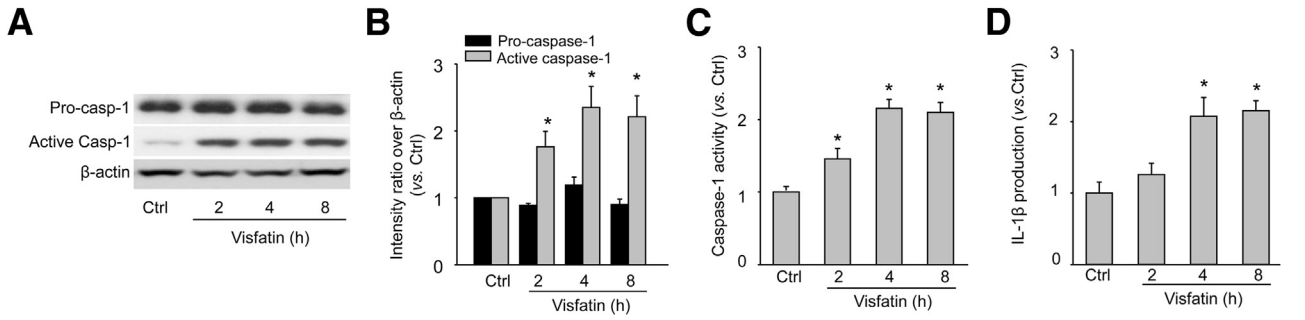

Figure 3 Visfatin activates caspase-1 and IL-1β production in MVECs. **A:** Western blot analysis shows the effect of visfatin on pro—caspase-1 and active caspase-1 expression. **B:** Summary of Western blot results. Summary of data for relative caspase-1 activity (**C**) and relative IL-1β production (**D**) compared with control. Data are expressed as means ± SEM; $n = 6$ (**C** and **D**). $^*P < 0.05$ versus control group.

increased caspase-1 activity (Figure 3C) and IL-1β release (Figure 3D) in MVECs. However, visfatin-induced caspase-1 activity and IL-1β production were attenuated by anti-visfatin antibody (Supplemental Figure S1). Collectively, these results indicated that visfatin induced formation and activation of the NLRP3 inflammasomes in MVECs.

Effects of *ASC* Gene Silencing or Caspase-1 Inhibition on Visfatin-Induced Inflammasome Activation

Knockdown of ASC mRNA level by ASC siRNA silencing in MVECs markedly inhibited visfatin-induced colocalization of NLRP3 with ASC or caspase-1 (Figure 4, A and B). Furthermore, visfatin-induced colocalization of NLRP3 with caspase-1 was attenuated in $Asc^{-/-}$ mice ECs (Supplemental Figure S2). Consistent with these findings, *ASC* gene silencing or blockade of caspase-1 activity by using WEHD almost completely blocked visfatin-induced increases in caspase-1 activity (Figure 4C) and IL-1β production (Figure 4D) in MVECs. In addition, visfatin-induced caspase-1 activity and IL-1β production in NLRP3 shRNA transfected MVECs (Supplemental Figure S3). Interestingly, 6 μg/mL adiponectin, the most abundant adipocyte protein with anti-inflammatory properties, had no effect on inflammasome formation, caspase-1 activity, and IL-1β production (Figure 4, A—D), indicating that this protective adipokine did not induce inflammasome formation and activation in MVECs.

Visfatin-Induced O_2^- Production in MVECs

Visfatin treatment significantly increased O_2^- production compared with control cells (Figure 5A). However, prior treatment with 1 mmol/L methyl-β-cyclodextrin [MCD; membrane raft (MR) disruptor] for 20 minutes and 0.1 mmol/L Tempol [reactive oxygen species (ROS) scavenger] for 20 minutes significantly attenuated the visfatin-induced O_2^- production. In contrast, thioredoxin-interacting protein (TXNIP) siRNA transfection did not alter O_2^- production induced by visfatin. These data suggested that visfatin activation of the NLRP3 inflammasomes might be through the MR-derived ROS production. Further, we examined whether the MR redox signaling pathway was involved in visfatin-induced NLRP3 inflammasome activation. We determined caspase-1 activity and IL-1β production in MVECs with or without prior treatment of MCD, Tempol, and TXNIP siRNA. Visfatin treatment significantly increased caspase-1 activity and IL-1β production compared with control cells (Figure 5, B and C). However, prior treatment with MCD, Tempol, and TXNIP siRNA significantly attenuated visfatin-induced caspase-1 activity and IL-1β production.

Efficiency of *in Vivo* Local Transfection of ASC shRNA into the Carotid Artery

We used an IVIS *in vivo* molecular imaging system to detect the expression of cotransfected luciferase gene, which ensures an efficient delivery of target gene into the mouse carotid artery (Figure 6A). The luciferase reporter gene was monitored in the carotid artery of the living mouse after the injection of plasmid mixed with microbubbles under ultrasound force. Starting on day 3, the expression of luciferase gene persisted for 2 weeks. As shown in an isolated carotid artery at day 6 after gene delivery, the reporter gene luciferase was specifically expressed on the LCA but not on the right carotid artery (Figure 6B). Immunohistochemical analyses indicated that ASC expression in the carotid artery was effectively inhibited even after 2 weeks of gene transfection (Figure 6C).

Morphological Analysis in PLCA of Mice with Visfatin Infusion

We next tested whether visfatin-induced inflammasome activation in ECs might affect neointimal expansion in mice with partially ligated carotid artery (PLCA). It was reported that IL-1β, a proinflammatory cytokine (an inflammasome product), plays a key role in the formation of neointimal lesion after PLCA in mice model[33] and that IL-1β was robustly increased in porcine coronary arteries after balloon injury.[33,34] Hence, we chose the PLCA model for *in vivo* studies. Morphological analysis indicated that visfatin infusion markedly increased the neointimal formation and

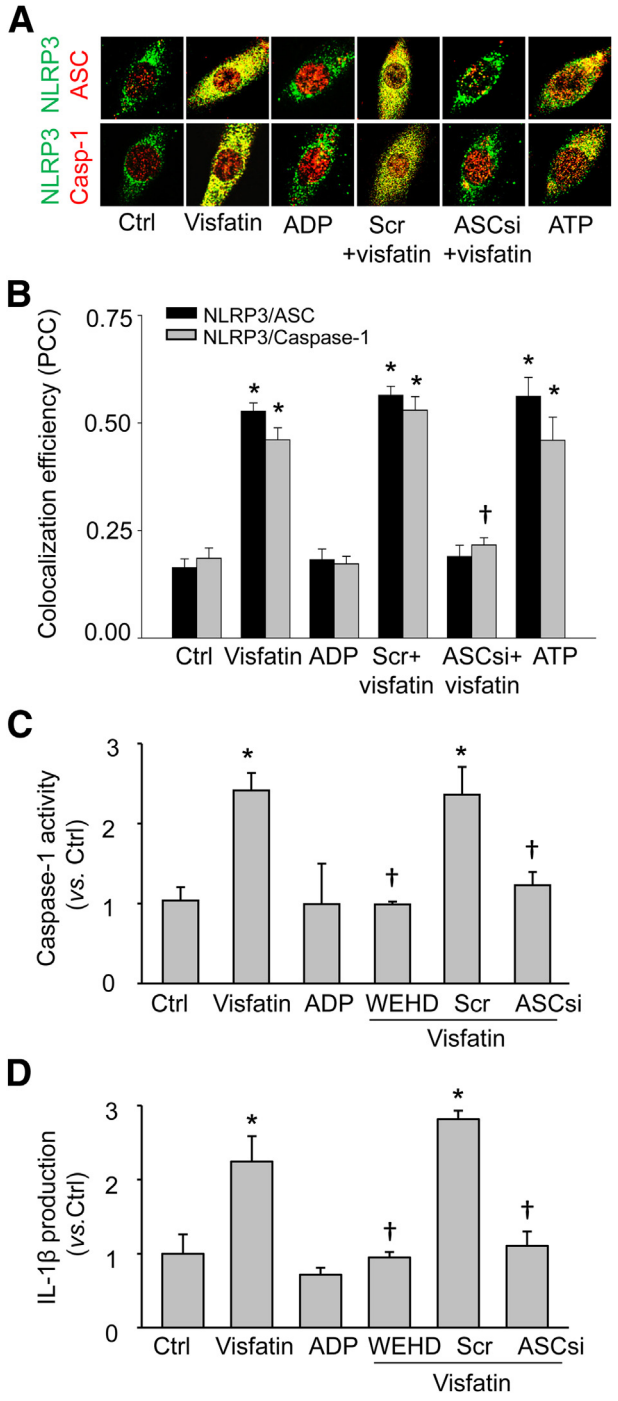

Figure 4 *ASC* gene silencing abolishes visfatin-induced NLRP3 inflammasome formation and activation in MVECs. **A:** Representative confocal fluorescence images show the colocalization of NLRP3 with ASC or NLRP3 with caspase-1. **B:** Data summary shows colocalization coefficiency of NLRP3 with ASC or caspase-1. Data summary shows relative caspase-1 activity (**C**) and relative IL-1β production (**D**) compared with control. Data are expressed as means ± SEM; $n = 6$. $^{*}P < 0.05$ versus untreated control group; $^{\dagger}P < 0.05$ (Scr + Visfatin versus ASCsi + Visfatin or visfatin versus WEHD + Visfatin). ADP, adiponectin; ASC si, Asc siRNA; ASCsi + visfatin, cells were transfected with ASC siRNA and then stimulated with visfatin; Casp-1, caspase-1; Scr + visfatin, cells were transfected with scramble RNA and then stimulated with visfatin; WEHD + visfatin, cells were pretreated with caspase-1 inhibitor WEHD and then stimulated with visfatin.

intima/media ratio in the PLCA model compared with vehicle-infused control mice (Figure 7, A and B). However, such visfatin-induced neointimal formation and increased intima/media ratio was significantly reduced by caspase-1 inhibitor WEHD, local carotid transfection of ASC shRNA, or in $Asc^{-/-}$ mice (Figure 7, A and B). Further, we tested whether such damage was directly induced by visfatin by immunohistochemical analysis and detected the visfatin expression in arteries. Visfatin penetrated into the intima section during infusion (Figure 7, C and D). This might directly switch on the intracellular inflammatory response, leading to further damage.

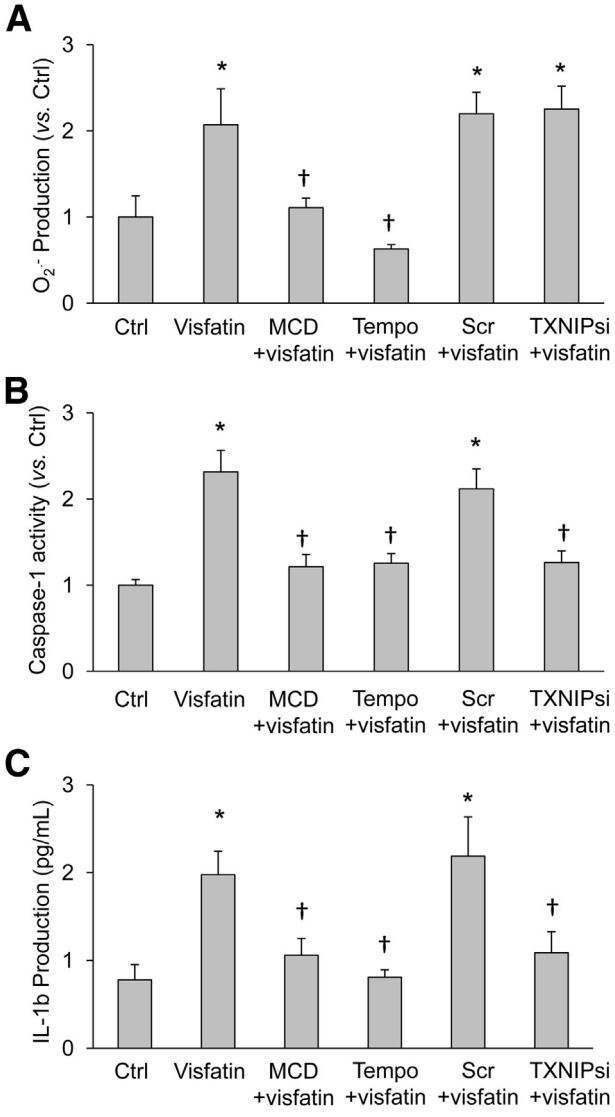

Figure 5 Effect of inhibition of MR-Redox signaling and TXNIP on visfatin-induced NLRP3 inflammasomes formation in MVECs. Data summary shows O_2^- production (**A**), caspase-1 activity (**B**), and IL-1β production (**C**) in MVECs with or without stimulation of visfatin. Data are expressed as means ± SEM; $n = 6$. $^{*}P < 0.05$ versus Ctrl group; $^{\dagger}P < 0.05$ versus visfatin group. MCD, methyl-β-cyclodextrin; Scram, scrambled siRNA; Tempo, 4-hydroxyl-tetramethylpiperidin-oxyl; TXNIP si, TXNIP siRNA.

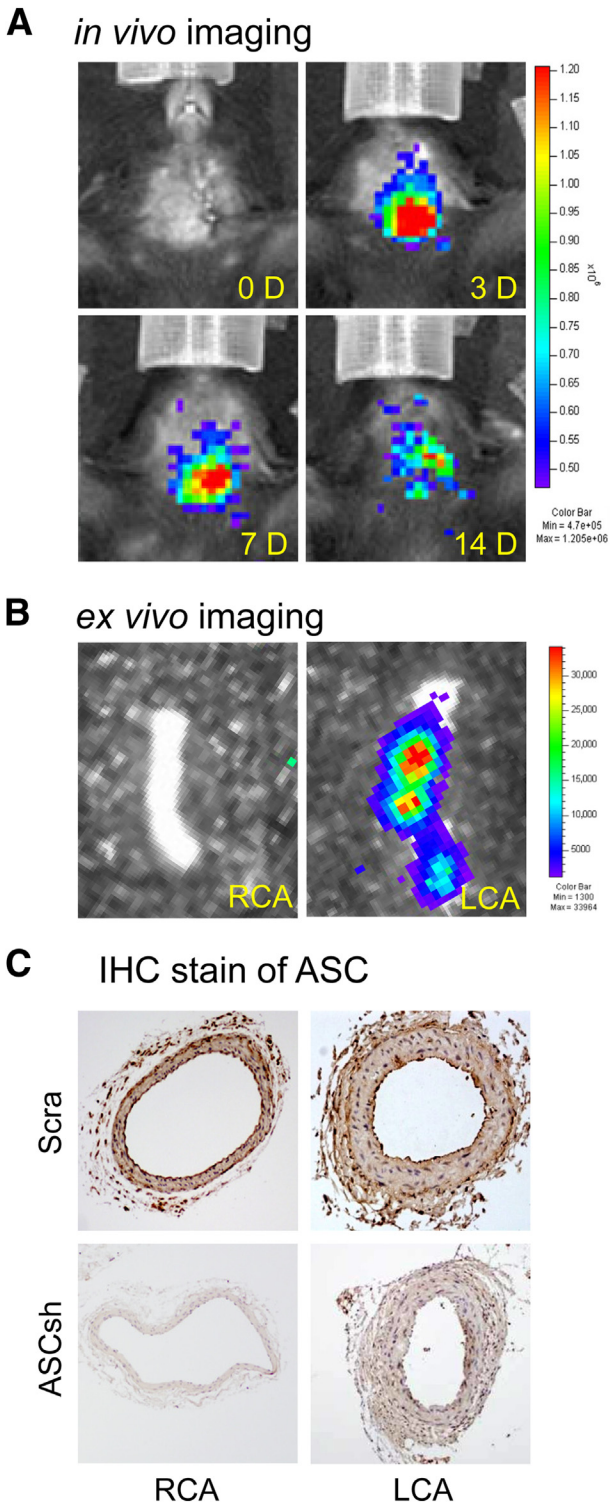

Figure 6 *In vivo* and *in vitro* determination of ASC shRNA transfection efficiency in the carotid artery. ASC shRNA (ASC sh) and luciferase cDNA plasmids were locally delivered into the LCA by using an ultrasound microbubble method. **A:** Daily imaging confirmation of gene transfection by detection of cotransfected luciferase gene expression by using an IVIS *in vivo* molecular imaging system. **B:** Localization of luciferase gene expression in isolated carotid arteries at day 6 after gene delivery. **C:** Immunohistochemical analysis of ASC expression in carotid arteries from mice with ASC shRNA transfection and partial ligation at the left artery for 2 weeks of visfatin administration. LCA, left carotid artery; RCA, right carotid artery; Scra, scrambled siRNA.

Inflammasome Formation and Activation in PLCA with Visfatin Infusion

Colocalization of NLRP3 with ASC or caspase-1 was barely observed in vehicle-infused control mice with PLCA (Figure 8, A and C). However, when these mice with PLCA were infused with visfatin, colocalization of NLRP3 with ASC or caspase-1 was significantly increased as indicated by intense yellow spots or patches in the intima of the arterial wall. The Pearson correlation coefficient of NLRP3 with ASC or caspase-1 showed the quantitative colocalization of NLRP3 with ASC (Figure 8B) or NLRP3 with caspase-1 (Figure 8D) in carotid arteries of mice. The colocalization of NLRP3 with ASC or caspase-1 suggests the formation of inflammasomes in the endothelium of PLCA in mice with visfatin administration. Moreover, ASC shRNA transfection or *ASC* gene deletion substantially suppressed and caspase-1 inhibition markedly attenuated the visfatin-induced colocalization of NLRP3 with ASC or caspase-1 in carotid arteries, suggesting that genetic or pharmacological interventions that target inflammasome components could block the visfatin-induced inflammasome formation in the endothelium of PLCA.

Immunohistochemical studies indicated that no IL-1β expression was detected in PLCA from vehicle-infused mice (Figure 9, A and B). However, visfatin-infused mice had a marked increase in IL-1β expression in the intima layer of PLCA. Such visfatin-induced IL-1β expression in the intima was abolished by the caspase-1 inhibitor WEHD, local carotid transfection of ASC shRNA, or *ASC* gene deletion.

Increased Inflammasome Formation and Activation in Obese Mice

In addition, we tested the role of NLRP3 inflammasomes in mice fed a HFD. We observed that a HFD significantly increased the plasma visfatin concentration compared with control mice (Supplemental Figure S4). WEHD treatment had no effect on plasma visfatin concentration. With the use of confocal microscopy, we observed that, under control condition, NLRP3 barely colocalized with caspase-1 in ND-fed mice, whereas in HFD-fed mice, we observed increased colocalization of NLRP3 with caspase-1 as indicated by intense yellow spots or patches in the intima of the arterial wall. Such colocalization suggests the formation of NLRP3 inflammasomes in coronary arterial endothelium in mice. Importantly, caspase-1 inhibition attenuated the HFD-induced colocalization of NLRP3 with caspase-1 in carotid arteries. Further, immunohistochemical analysis indicated that IL-1β expression was barely detected in coronary arteries of ND-fed mice. HFD markedly increased the IL-1β expression in endothelium layer of coronary arteries (increased brown staining in the intima). However, caspase-1 inhibition significantly attenuated the HFD-induced increase in IL-1β expression (Supplemental Figure S4).

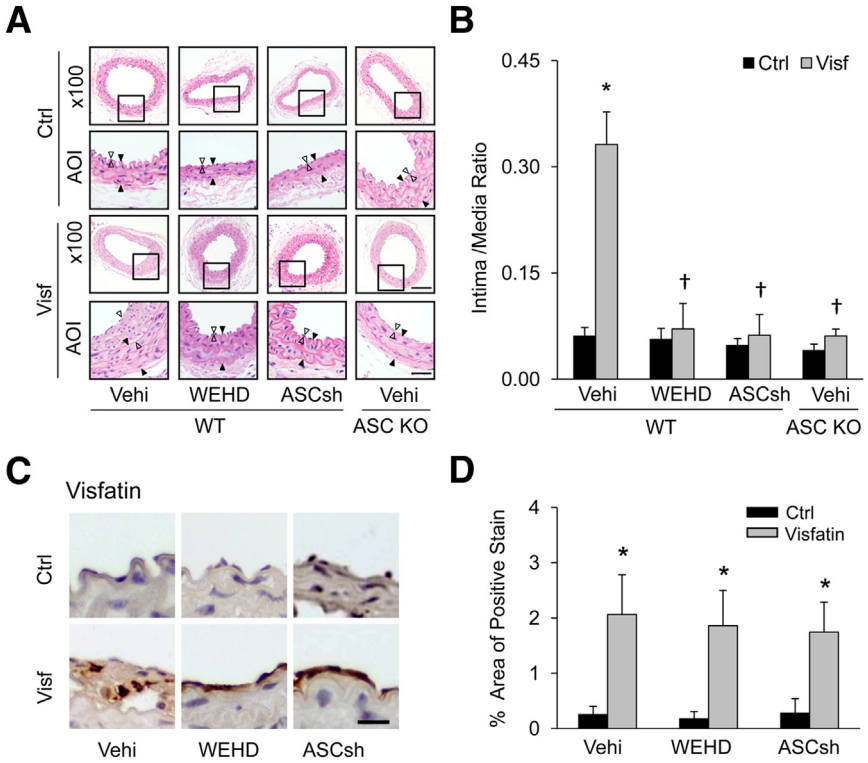

Figure 7 Visfatin infusion enhances neointimal formation in PLCA. WT mice were intravenously infused by vehicle or visfatin and were treated with vehicle (Ctrl) or caspase-1 inhibitor WEHD or transfected with ASC shRNA for 2 weeks after the partial ligation of the left artery. ASC KO mice were intravenously infused by vehicle or visfatin for 2 weeks after partial ligation of the left artery. **A:** Photomicrographs of PLCA 2 weeks after visfatin i.v. infusion (H&E staining). AOI: the media area (**black arrowheads**) and the intima area (**white arrowheads**). **B:** Quantitative analysis of vascular lesions in PLCA represented by the ratio between intima and media. **C:** Representative immunohistochemical images of visfatin expression in endothelial layer of PLCA. **D:** Quantitative analysis of positive stain of visfatin in intima section. Data are expressed as means ± SEM; $n = 6$ mice per group. $^{*}P < 0.05$ versus vehicle control group; $^{\dagger}P < 0.05$ versus visfatin group. Scale bars: 50 μm (**A**, ×100 images); 20 μm (**A**, AOI images); 5 μm (**C**). AOI, area of interest; Ctrl, control; KO, knockout; Vehi, vehicle; Visf, visfatin; WT, wild-type.

Discussion

The present study indicated that visfatin induced formation and activation of NLRP3 inflammasomes both *in vitro* and *in vivo*. In cultured MVECs, visfatin induced aggregation of NLRP3 inflammasome components, activation of caspase-1, and production of IL-1β. Our animal experiments demonstrated that visfatin infusion significantly increased inflammasome formation, caspase-1 activity, and IL-1β production in PLCAs, which were almost completely blocked by caspase-1 inhibition or *Asc* gene inhibition. These results suggest that the formation and activation of NLRP3 inflammasomes by visfatin may be an important initiating mechanism to turn on the endothelial inflammatory response, leading to carotid inflammation and endothelial dysfunction during obesity.

Visfatin, an adipokine involved in pro-inflammatory responses,[27] has been implicated in a wide range of inflammatory disorders in obesity and associated cardiovascular diseases.[23,24,35] Visfatin has been demonstrated as contributor to endothelial dysfunction through the up-regulation of NF-κB activation in ECs,[36] which is an important step for NLRP3 inflammasome-mediated IL-1β production.[27,37] NLRP3 inflammasome activation is known to cause caspase-1 activation and cleavage of pro−IL-1β and pro-18 into their bioactive form, namely, IL-1β or IL-18. Therefore, the present study explored whether it is indeed involved in visfatin-induced IL-1β production and inflammatory responses. We first characterized the expression and activation of this inflammasome complex and found mRNA and protein expression of the three NLRP3 inflammasome molecules, namely NLRP3, ASC, and caspase-1, in MVECs. Importantly, visfatin stimulation induced the formation of NLRP3 inflammasomes in MVECs as shown by colocalization of NLRP3 with ASC or NLRP3 with caspase-1. Because inflammasomes form multimolecular oligomers with high-molecular weight, inflammasomes can be isolated and detected by SEC with Western blot analysis as described.[38] With the use of these approaches, we found that visfatin increased expression of NLRP3, ASC, and caspase-1 in high-molecular weight fractions (>600 kDa), which confirms the assembly of inflammasomes in MVECs. Moreover, biochemical analysis demonstrated that visfatin increased the caspase-1 activity and IL-1β production in MVECs. Thus, these results clearly show that the NLRP3 inflammasomes are present and functioning in ECs and that visfatin stimulation can lead to their activation. Consistently, recent studies also demonstrated the activation of NLRP3 inflammasomes in ECs under different conditions such as lipopolysaccharide and interferon-γ stimulation, acetaminophen treatment, or hemorrhagic shock.[39–42] Although these reports showed that NLRP3 and other inflammasomes can be activated in ECs under different pathological conditions, the results from the present study provide the first experimental evidence that adipokine visfatin can activate NLRP3 inflammasomes in ECs, which may be an important pathogenic mechanism responsible for endothelial inflammation during obesity.

The present study further examined the mechanism of action of visfatin-induced NLRP3 inflammasome activation in MVECs. Our recent studies demonstrated that visfatin is an important factor to activate NADPH oxidase-derived ROS production through MR redox signaling platforms in

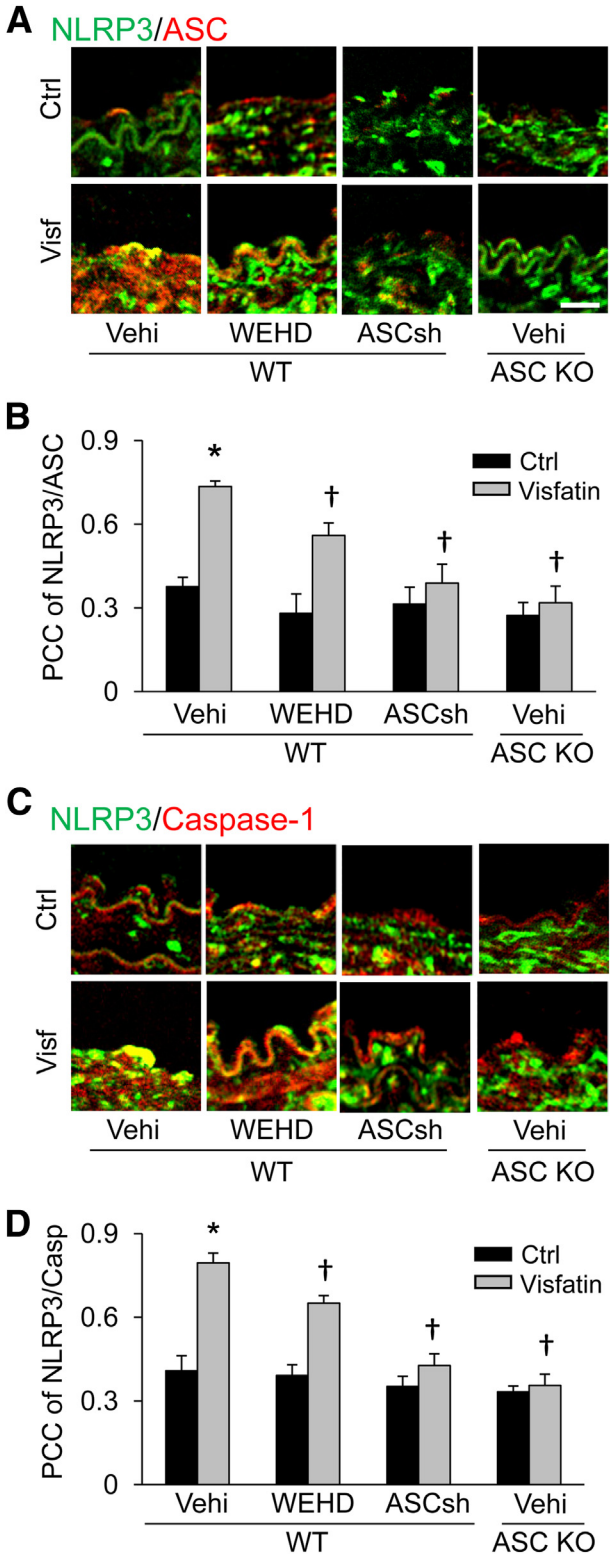

Figure 8 Visfatin induces the NLRP3 inflammasome formation in PLCA. Representative confocal fluorescence images show the colocalization of NLRP3 with ASC (**A**) or caspase-1 (**C**) in the intima of PLCA. Data summary shows the colocalization efficiency of NLRP3 with ASC (**B**) or caspase-1 (**D**). Data are expressed as means ± SEM; $n = 6$ mice per group. $^{*}P < 0.05$ versus vehicle control group; $^{\dagger}P < 0.05$ versus visfatin group. Scale bars: 10 μm (**A** and **C**). Ctrl, control; KO, knockout; PCC, Pearson correlation coefficient; Vehi, vehicle; WT, wild-type.

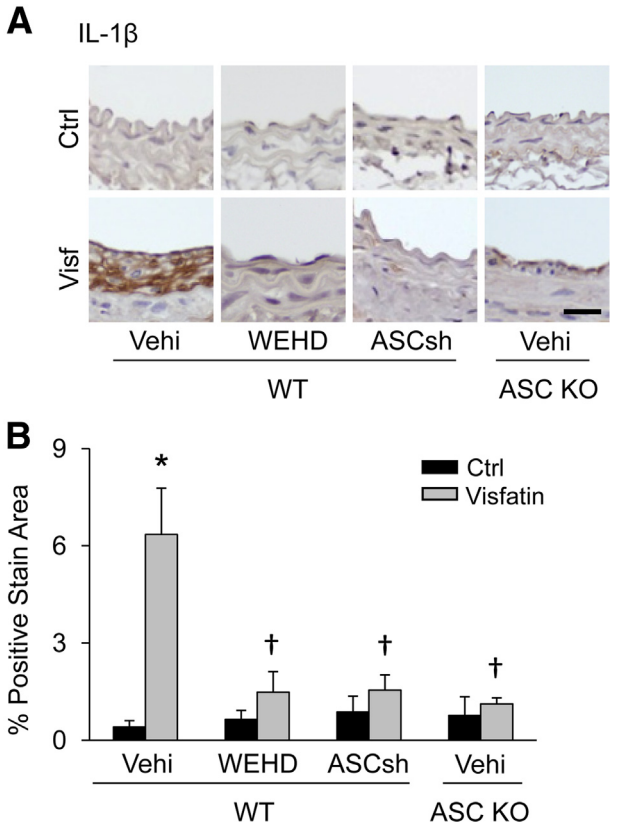

Figure 9 Visfatin increases the IL-1β production in PLCA. **A:** Representative immunohistochemical images show IL-1β-positive stains in the intima of PLCA. **B:** Quantitative analysis of positive stain of IL-1β in intima section. Data are expressed as means ± SEM; $n = 6$ mice per group. $^{*}P < 0.05$ versus vehicle control group; $^{\dagger}P < 0.05$ versus visfatin group. Scale bar = 10 μm. Ctrl, control; KO, knockout; Vehi, vehicle; WT, wild-type.

ECs.[28,29] It has been proposed that ROS act on a target upstream of the NLRP3 inflammasome and indirectly cause its activation.[43–45] However, the pathway that links ROS to the inflammasome remains largely unknown. A recent study showed that NLRP3 interaction with TXNIP whereby inflammasome activators such as uric acid crystals induced the dissociation of TXNIP from thioredoxin in a ROS-sensitive manner and allowed it to bind NLRP3.[46] In the present study, we confirmed that visfatin-induced ROS production in MVECs, which was blocked by disrupting MR redox signaling platforms (Figure 5A). Further, we demonstrated that visfatin-induced caspase-1 activation and IL-1β production were blocked by MR redox platform disruption, ROS scavenging, or *TXNIP* gene silencing (Figure 5, B and C). Thus, our data suggest that MR redox signaling platform-derived ROS could be an important mechanism to mediate visfatin-induced NLRP3 inflammasome activation in ECs via ROS-dependent release of TXNIP and consequent TXNIP-NLRP3 interaction.

To further explore the role of NLRP3 inflammasomes in mediating the action of visfatin *in vivo*, we locally modulated gene expression of ASC in mouse carotid artery and

observed changes in NLRP3 inflammasome colocalization in PLCA with visfatin infusion. To reach this goal, we combined an ultrasound technique and microbubble wrapping to introduce plasmids into coronary vascular beds. Several recent reports from our laboratory and by others have shown that the ultrasound-microbubble system is an effective method to deliver plasmids into cells of different organs *in vivo* with a transfection rate >90%.[47–50] Combination of the ultrasound technique and microbubble wrapping for introduction of plasmids greatly enhances transgene expression with a 300-fold increase over naked DNA alone without toxicity.[48,50] The present study by using *in vivo* molecular imaging demonstrated that plasmids (ASC shRNA plasmids cotransfected with luciferase cDNA plasmid) were successfully delivered into the LCA and cotransfected luciferase expression persisted for up to 2 weeks. Such local gene silencing efficiently blocked ASC expression in PLCA (Figure 6C). However, the local gene silencing in mouse carotid artery had trivial or insignificant decreases in visfatin expression levels in intima of visfatin-infused PLCA (Figure 7D), suggesting that inhibition of ASC expression by this local gene silencing is only effective and limited to PLCA.

Although the strategies used to inhibit *Asc* in mice were not endothelial specific, confocal fluorescence microscopy and immunohistochemical analysis revealed that such local *Asc* gene silencing or *Asc* gene deletion substantially abolished the visfatin-induced NLRP3 inflammasome formation and IL-1β production in the endothelium of PLCA. Inhibition of caspase-1 activity also markedly attenuated inflammasome formation and IL-1β production in the endothelium of PLCA. Taken together, our data provided strong *in vivo* evidence that visfatin is an effective inflammasome activator that leads to local inflammation in the vasculature.

The present study further demonstrated that visfatin enhanced the neointimal formation in PLCA, which was blocked by local silencing of *Asc* gene or caspase-1 inhibition in the carotid artery. These data imply that visfatin-induced endothelial inflammasome activation may play a crucial role in initiation of endothelial dysfunction and vascular injury. The present study did not aim to define the precise mechanism of how visfatin-induced NLRP3 inflammasome activation leads to endothelial dysfunction or injury. It should be noted that visfatin could also be up-regulated by IL-1β.[51,52] In this regard, it is possible that elevation of plasma visfatin during obesity may initiate NLRP3 inflammasome activation in ECs to release a small amount of IL-1β. This small amount of IL-1β could then function in a paracrine or autocrine fashion to increase massive visfatin expression in the vasculature, which may result in a vicious cycle that amplifies the inflammasome-mediated responses that lead to endothelial dysfunction or injury. Targeting this visfatin-inflammasome machinery at the stage of its assembling or activation may be a novel therapeutic strategy to prevent the development of endothelial dysfunction or injury during obesity.

In summary, the present study revealed a new triggering mechanism of visfatin-induced inflammation that is characterized by the formation and activation of NLRP3 inflammasomes in ECs *in vitro* and *in vivo*. This activation of NLRP3 inflammasomes may represent a novel early event that leads to endothelial dysfunction and injury, initiating atherosclerosis during obesity.

Supplemental Data

Supplemental material for this article can be found at *http://dx.doi.org/10.1016/j.ajpath.2014.01.032*.

References

1. Hubert HB, Feinleib M, McNamara PM, Castelli WP: Obesity as an independent risk factor for cardiovascular disease: a 26-year follow-up of participants in the Framingham Heart Study. Circulation 1983, 67:968–977
2. Duewell P, Kono H, Rayner KJ, Sirois CM, Vladimer G, Bauernfeind FG, Abela GS, Franchi L, Nunez G, Schnurr M, Espevik T, Lien E, Fitzgerald KA, Rock KL, Moore KJ, Wright SD, Hornung V, Latz E: NLRP3 inflammasomes are required for atherogenesis and activated by cholesterol crystals. Nature 2010, 464:1357–1361
3. Masters SL, Latz E, O'Neill LA: The inflammasome in atherosclerosis and type 2 diabetes. Sci Transl Med 2011, 3:81ps17
4. Ross R: Atherosclerosis–an inflammatory disease. N Engl J Med 1999, 340:115–126
5. Libby P: Inflammation in atherosclerosis. Nature 2002, 420:868–874
6. Hansson GK: Inflammation, atherosclerosis, and coronary artery disease. N Engl J Med 2005, 352:1685–1695
7. Wen H, Ting JP, O'Neill LA: A role for the NLRP3 inflammasome in metabolic diseases–did Warburg miss inflammation? Nat Immunol 2012, 13:352–357
8. Strowig T, Henao-Mejia J, Elinav E, Flavell R: Inflammasomes in health and disease. Nature 2012, 481:278–286
9. Martinon F, Mayor A, Tschopp J: The inflammasomes: guardians of the body. Annu Rev Immunol 2009, 27:229–265
10. Busso N, So A: Mechanisms of inflammation in gout. Arthritis Res Ther 2010, 12:206
11. Stienstra R, Tack CJ, Kanneganti TD, Joosten LA, Netea MG: The inflammasome puts obesity in the danger zone. Cell Metab 2012, 15:10–18
12. Mariathasan S, Newton K, Monack DM, Vucic D, French DM, Lee WP, Roose-Girma M, Erickson S, Dixit VM: Differential activation of the inflammasome by caspase-1 adaptors ASC and Ipaf. Nature 2004, 430:213–218
13. Martinon F, Petrilli V, Mayor A, Tardivel A, Tschopp J: Gout-associated uric acid crystals activate the NALP3 inflammasome. Nature 2006, 440:237–241
14. Halle A, Hornung V, Petzold GC, Stewart CR, Monks BG, Reinheckel T, Fitzgerald KA, Latz E, Moore KJ, Golenbock DT: The NALP3 inflammasome is involved in the innate immune response to amyloid-beta. Nat Immunol 2008, 9:857–865
15. Zheng Y, Gardner SE, Clarke MC: Cell death, damage-associated molecular patterns, and sterile inflammation in cardiovascular disease. Arterioscler Thromb Vasc Biol 2011, 31:2781–2786
16. Dinarello CA, Donath MY, Mandrup-Poulsen T: Role of IL-1beta in type 2 diabetes. Curr Opin Endocrinol Diabetes Obes 2010, 17:314–321
17. Rodriguez G, Mago N, Rosa F: [Role of inflammation in atherogenesis]. Spanish. Invest Clin 2009, 50:109–129

18. Rathinam VA, Vanaja SK, Fitzgerald KA: Regulation of inflammasome signaling. Nat Immunol 2012, 13:333–342
19. Wen H, Gris D, Lei Y, Jha S, Zhang L, Huang MT, Brickey WJ, Ting JP: Fatty acid-induced NLRP3-ASC inflammasome activation interferes with insulin signaling. Nat Immunol 2011, 12:408–415
20. Samal B, Sun Y, Stearns G, Xie C, Suggs S, McNiece I: Cloning and characterization of the cDNA encoding a novel human pre-B-cell colony-enhancing factor. Mol Cell Biol 1994, 14:1431–1437
21. Fukuhara A, Matsuda M, Nishizawa M, Segawa K, Tanaka M, Kishimoto K, Matsuki Y, Murakami M, Ichisaka T, Murakami H, Watanabe E, Takagi T, Akiyoshi M, Ohtsubo T, Kihara S, Yamashita S, Makishima M, Funahashi T, Yamanaka S, Hiramatsu R, Matsuzawa Y, Shimomura I: Visfatin: a protein secreted by visceral fat that mimics the effects of insulin. Science 2005, 307:426–430
22. Adeghate E: Visfatin: structure, function and relation to diabetes mellitus and other dysfunctions. Curr Med Chem 2008, 15: 1851–1862
23. Dahl TB, Yndestad A, Skjelland M, Oie E, Dahl A, Michelsen A, Damas JK, Tunheim SH, Ueland T, Smith C, Bendz B, Tonstad S, Gullestad L, Froland SS, Krohg-Sorensen K, Russell D, Aukrust P, Halvorsen B: Increased expression of visfatin in macrophages of human unstable carotid and coronary atherosclerosis: possible role in inflammation and plaque destabilization. Circulation 2007, 115:972–980
24. Zhong M, Tan HW, Gong HP, Wang SF, Zhang Y, Zhang W: Increased serum visfatin in patients with metabolic syndrome and carotid atherosclerosis. Clin Endocrinol (Oxf) 2008, 69:878–884
25. Yilmaz MI, Saglam M, Carrero JJ, Qureshi AR, Caglar K, Eyileten T, Sonmez A, Cakir E, Yenicesu M, Lindholm B, Stenvinkel P, Axelsson J: Serum visfatin concentration and endothelial dysfunction in chronic kidney disease. Nephrol Dial Transplant 2008, 23:959–965
26. Spiroglou SG, Kostopoulos CG, Varakis JN, Papadaki HH: Adipokines in periaortic and epicardial adipose tissue: differential expression and relation to atherosclerosis. J Atheroscler Thromb 2010, 17: 115–130
27. Moschen AR, Kaser A, Enrich B, Mosheimer B, Theurl M, Niederegger H, Tilg H: Visfatin, an adipocytokine with proinflammatory and immunomodulating properties. J Immunol 2007, 178: 1748–1758
28. Xia M, Zhang C, Boini KM, Thacker AM, Li PL: Membrane raft-lysosome redox signalling platforms in coronary endothelial dysfunction induced by adipokine visfatin. Cardiovasc Res 2011, 89:401–409
29. Boini KM, Zhang C, Xia M, Han WQ, Brimson C, Poklis JL, Li PL: Visfatin-induced lipid raft redox signaling platforms and dysfunction in glomerular endothelial cells. Biochim Biophys Acta 2010, 1801: 1294–1304
30. Nam D, Ni CW, Rezvan A, Suo J, Budzyn K, Llanos A, Harrison D, Giddens D, Jo H: Partial carotid ligation is a model of acutely induced disturbed flow, leading to rapid endothelial dysfunction and atherosclerosis. Am J Physiol Heart Circ Physiol 2009, 297:H1535–H1543
31. Merino H, Parthasarathy S, Singla DK: Partial ligation-induced carotid artery occlusion induces leukocyte recruitment and lipid accumulation–a shear stress model of atherosclerosis. Mol Cell Biochem 2013, 372:267–273
32. Boini KM, Zhang C, Xia M, Poklis JL, Li PL: Role of sphingolipid mediator ceramide in obesity and renal injury in mice fed a high-fat diet. J Pharmacol Exp Ther 2010, 334:839–846
33. Chamberlain J, Evans D, King A, Dewberry R, Dower S, Crossman D, Francis S: Interleukin-1beta and signaling of interleukin-1 in vascular wall and circulating cells modulates the extent of neointima formation in mice. Am J Pathol 2006, 168:1396–1403
34. Chamberlain J, Gunn J, Francis S, Holt C, Crossman D: Temporal and spatial distribution of interleukin-1 beta in balloon injured porcine coronary arteries. Cardiovasc Res 1999, 44:156–165
35. Reimann M, Ziemssen T, Huisman HW, Schutte R, Malan L, Van Rooyen JM, Boger RH, Malan NT, Schutte AE: Ethnic-specific correlations of visfatin with circulating markers of endothelial inflammation and function. Obesity (Silver Spring) 2009, 17:2210–2215
36. Mizushima N, Levine B, Cuervo AM, Klionsky DJ: Autophagy fights disease through cellular self-digestion. Nature 2008, 451:1069–1075
37. Park BS, Jin SH, Park JJ, Park JW, Namgoong IS, Kim YI, Lee BJ, Kim JG: Visfatin induces sickness responses in the brain. PLoS One 2011, 6:e15981
38. Abulafia DP, de Rivero Vaccari JP, Lozano JD, Lotocki G, Keane RW, Duetruch WD: Inhibition of the inflammasome complex reduces the inflammatory response after thromboembolic stroke in mice. J Cereb Blood Flow Metab 2009, 29:534–544
39. Xiang M, Shi X, Li Y, Xu J, Yin L, Xiao G, Scott MJ, Billiar TR, Wilson MA, Fan J: Hemorrhagic shock activation of NLRP3 inflammasome in lung endothelial cells. J Immunol 2011, 187:4809–4817
40. Imaeda AB, Watanabe A, Sohail MA, Mahmood S, Mohamadnejad M, Sutterwala FS, Flavell RA, Mehal WZ: Acetaminophen-induced hepatotoxicity in mice is dependent on Tlr9 and the Nalp3 inflammasome. J Clin Invest 2009, 119:305–314
41. Yin Y, Yan Y, Jiang X, Mai J, Chen NC, Wang H, Yang XF: Inflammasomes are differentially expressed in cardiovascular and other tissues. Int J Immunopathol Pharmacol 2009, 22:311–322
42. Yazdi AS, Drexler SK, Tschopp J: The role of the inflammasome in nonmyeloid cells. J Clin Immunol 2010, 30:623–627
43. Cruz CM, Rinna A, Forman HJ, Ventura AL, Persechini PM, Ojcius DM: ATP activates a reactive oxygen species-dependent oxidative stress response and secretion of proinflammatory cytokines in macrophages. J Biol Chem 2007, 282:2871–2879
44. Dostert C, Petrilli V, Van Bruggen R, Steele C, Mossman BT, Tschopp J: Innate immune activation through Nalp3 inflammasome sensing of asbestos and silica. Science 2008, 320:674–677
45. Tschopp J, Schroder K: NLRP3 inflammasome activation: the convergence of multiple signalling pathways on ROS production? Nat Rev Immunol 2010, 10:210–215
46. Zhou R, Tardivel A, Thorens B, Choi I, Tschopp J: Thioredoxin-interacting protein links oxidative stress to inflammasome activation. Nat Immunol 2010, 11:136–140
47. Yi F, Xia M, Li N, Zhang C, Tang L, Li PL: Contribution of guanine nucleotide exchange factor Vav2 to hyperhomocysteinemic glomerulosclerosis in rats. Hypertension 2009, 53:90–96
48. Bekeredjian R, Chen S, Frenkel PA, Grayburn PA, Shohet RV: Ultrasound-targeted microbubble destruction can repeatedly direct highly specific plasmid expression to the heart. Circulation 2003, 108: 1022–1026
49. Chen S, Shohet RV, Bekeredjian R, Frenkel P, Grayburn PA: Optimization of ultrasound parameters for cardiac gene delivery of adenoviral or plasmid deoxyribonucleic acid by ultrasound-targeted microbubble destruction. J Am Coll Cardiol 2003, 42:301–308
50. Tsunoda S, Mazda O, Oda Y, Iida Y, Akabame S, Kishida T, Shin-Ya M, Asada H, Gojo S, Imanishi J, Matsubara H, Yoshikawa T: Sonoporation using microbubble BR14 promotes pDNA/siRNA transduction to murine heart. Biochem Biophys Res Commun 2005, 336:118–127
51. Ognjanovic S, Bao S, Yamamoto SY, Garibay-Tupas J, Samal B, Bryant-Greenwood GD: Genomic organization of the gene coding for human pre-B-cell colony enhancing factor and expression in human fetal membranes. J Mol Endocrinol 2001, 26:107–117
52. Gosset M, Berenbaum F, Salvat C, Sautet A, Pigenet A, Tahiri K, Jacques C: Crucial role of visfatin/pre-B cell colony-enhancing factor in matrix degradation and prostaglandin E2 synthesis in chondrocytes: possible influence on osteoarthritis. Arthritis Rheum 2008, 58:1399–1409